A sparse regularization approach for ultrafast ultrasound imaging

Rafael Carrillo[1], **Adrien Besson**[13], Miaomiao Zhang[2], Denis Friboulet[2], Yves Wiaux[3], Jean-Philippe Thiran[1] and Olivier Bernard[2]

[1]Signal Processing Laboratory (LTS5)
École Polytechnique Fédérale de Lausanne, Switzerland

[2]CREATIS
University of Lyon, France

[3]Institute of Sensors, Signals and Systems
Heriot-Watt University, Scotland

IEEE International Ultrasonics Symposium, October 2015

Outline

Outline

Ultrafast Ultrasound imaging

ÉCOLE POLYTECHNIQUE
FÉDÉRALE DE LAUSANNE

Ultrafast Ultrasound Imaging
Principle

Ultrafast Ultrasound imaging

- Emission of one single plane wave (PW) or few steered PWs
  - Can reach more than thousands frames per second

Ultrafast Ultrasound imaging

- Emission of one single plane wave (PW) or few steered PWs
  - Can reach more than thousands frames per second
  - Lower image quality than classical method

Ultrafast Ultrasound Imaging
Principle

Ultrafast Ultrasound imaging

- Emission of one single plane wave (PW) or few steered PWs
  - Can reach more than thousands frames per second
  - Lower image quality than classical method

State of the art approaches

Ultrafast Ultrasound imaging

- Emission of one single plane wave (PW) or few steered PWs
  - Can reach more than thousands frames per second
  - Lower image quality than classical method

State of the art approaches

- Spatial based approaches: [Montaldo *et al.*, 2009]

Ultrafast Ultrasound imaging

- Emission of one single plane wave (PW) or few steered PWs
  - Can reach more than thousands frames per second
  - Lower image quality than classical method

State of the art approaches

- Spatial based approaches: [Montaldo *et al.*, 2009]
- **Fourier based approaches:** [Lu *et al.*, 1997] [Garcia *et al.*, 2013] [Bernard *et al.*, 2014]

Ultrafast Ultrasound Imaging
Principle

Ultrafast Ultrasound imaging

- Emission of one single plane wave (PW) or few steered PWs
  - Can reach more than thousands frames per second
  - Lower image quality than classical method

State of the art approaches

- Spatial based approaches: [Montaldo *et al.*, 2009]
- **Fourier based approaches:** [Lu *et al.*, 1997] [Garcia *et al.*, 2013] [Bernard *et al.*, 2014]

Ultrasound Fourier slice Beamforming (UFSB) - General scheme

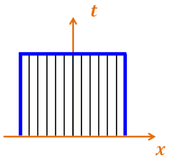

Backscattered echoes

Ultrafast Ultrasound Imaging
Principle

Ultrafast Ultrasound imaging

- Emission of one single plane wave (PW) or few steered PWs
  - Can reach more than thousands frames per second
  - Lower image quality than classical method

State of the art approaches

- Spatial based approaches: [Montaldo *et al.*, 2009]
- **Fourier based approaches:** [Lu *et al.*, 1997] [Garcia *et al.*, 2013] [Bernard *et al.*, 2014]

Ultrasound Fourier slice Beamforming (UFSB) - General scheme

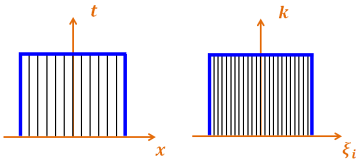

Backscattered echoes Radial Fourier samples

ÉCOLE POLYTECHNIQUE FÉDÉRALE DE LAUSANNE

Ultrafast Ultrasound Imaging
Principle

Ultrafast Ultrasound imaging

- Emission of one single plane wave (PW) or few steered PWs
  - Can reach more than thousands frames per second
  - Lower image quality than classical method

State of the art approaches

- Spatial based approaches: [Montaldo *et al.*, 2009]
- **Fourier based approaches:** [Lu *et al.*, 1997] [Garcia *et al.*, 2013] [Bernard *et al.*, 2014]

Ultrasound Fourier slice Beamforming (UFSB) - General scheme

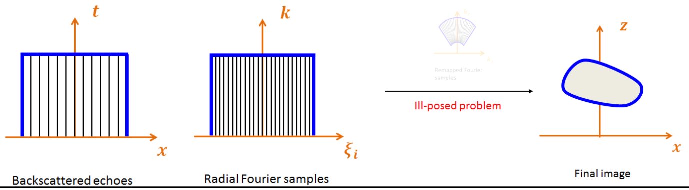

Outline

UFSB poses an inverse problem

A sparse regularization approach to US imaging
The two pillars

UFSB poses an inverse problem

$$\boldsymbol{y} = \Phi \boldsymbol{r} + \boldsymbol{n}, \text{ with } \Phi \text{ ill-posed}$$

UFSB poses an inverse problem

$$\boldsymbol{y} = \Phi \boldsymbol{r} + \boldsymbol{n}, \text{ with } \Phi \text{ ill-posed}$$

- $\boldsymbol{y}$ are the radial Fourier samples, $\boldsymbol{r}$ is the desired image, $\boldsymbol{n}$ is the noise
- Measurement operator: Φ is the 2D Non-Uniform Fourier Transform

A sparse regularization approach to US imaging
The two pillars

UFSB poses an inverse problem

$$\boldsymbol{y} = \Phi \boldsymbol{r} + \boldsymbol{n}, \text{ with } \Phi \text{ ill-posed}$$

- $\boldsymbol{y}$ are the radial Fourier samples, $\boldsymbol{r}$ is the desired image, $\boldsymbol{n}$ is the noise
- Measurement operator: Φ is the 2D Non-Uniform Fourier Transform

US images are sparse in an appropriate model

UFSB poses an inverse problem

$$\boldsymbol{y} = \Phi \boldsymbol{r} + \boldsymbol{n}, \text{ with } \Phi \text{ ill-posed}$$

- $\boldsymbol{y}$ are the radial Fourier samples, $\boldsymbol{r}$ is the desired image, $\boldsymbol{n}$ is the noise
- Measurement operator: Φ is the 2D Non-Uniform Fourier Transform

US images are sparse in an appropriate model

- Several models already studied: Wavelet basis, Wave atoms frame, Fourier basis

A sparse regularization approach to US imaging
The two pillars

UFSB poses an inverse problem

$$\boldsymbol{y} = \Phi \boldsymbol{r} + \boldsymbol{n}, \text{ with } \Phi \text{ ill-posed}$$

- $\boldsymbol{y}$ are the radial Fourier samples, $\boldsymbol{r}$ is the desired image, $\boldsymbol{n}$ is the noise
- Measurement operator: Φ is the 2D Non-Uniform Fourier Transform

US images are sparse in an appropriate model

- Several models already studied: Wavelet basis, Wave atoms frame, Fourier basis
- Sparsity averaging model (SARA) Ψ used: [Carrillo *et al.*, 2012]
  - Concatenation of wavelet basis: $\Psi = \frac{1}{\sqrt{q}}[\Psi_1, ..., \Psi_q]$
  - In the study: $q = 8$, Daubechies wavelet as mother function

Reconstruction problem

Reconstruction problem

- The image is recovered by solving the inverse problem:

$$\min_{\bar{\boldsymbol{r}} \in \mathbb{C}^N} \|\Psi^H \bar{\boldsymbol{r}}\|_1 \text{ subject to } \|\boldsymbol{y} - \Phi \bar{\boldsymbol{r}}\|_2 \leq \epsilon$$

- Non-linear but Convex problem

A sparse regularization approach to US imaging
The image reconstruction

Reconstruction problem

- The image is recovered by solving the inverse problem:

$$\min_{\bar{\boldsymbol{r}} \in \mathbb{C}^N} \|\Psi^H \bar{\boldsymbol{r}}\|_1 \text{ subject to } \|\boldsymbol{y} - \Phi \bar{\boldsymbol{r}}\|_2 \leq \epsilon$$

- Non-linear but Convex problem

Reconstruction algorithm

Reconstruction problem

- The image is recovered by solving the inverse problem:

$$\min_{\bar{\boldsymbol{r}} \in \mathbb{C}^N} \|\Psi^H \bar{\boldsymbol{r}}\|_1 \text{ subject to } \|\boldsymbol{y} - \Phi \bar{\boldsymbol{r}}\|_2 \leq \epsilon$$

- Non-linear but Convex problem

Reconstruction algorithm

- ADMM algorithm [Boyd *et al.*, 2010]
- Golden section search to find the best value of ϵ

Outline

Experimental study
Protocol

Numerical simulations

- Based on Field II software [Jensen, 1991]
- Contrast to Noise ratio (CNR)

Experimental data

- UlaOp ultrasound scanner with linear probe
- Spatial resolution

Comparisons

- Fourier based approaches: Lu, Garcia and Bernard
- Spatial based approaches: Montaldo

Contrast to Noise Ratio

- Measured from numerical simulations
  - 2 x 2 cm phantom with high density of scatterers
  - 8mm-diameter anechoic lesion centered inside the phantom

Contrast to Noise Ratio

- Measured from numerical simulations
  - 2 x 2 cm phantom with high density of scatterers
  - 8mm-diameter anechoic lesion centered inside the phantom

Reconstruction results

Contrast to Noise Ratio

- Measured from numerical simulations
  - 2 x 2 cm phantom with high density of scatterers
  - 8mm-diameter anechoic lesion centered inside the phantom

Reconstruction results

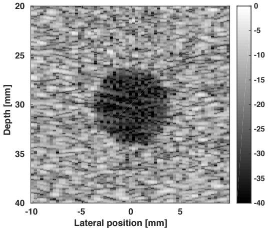

(a) Classic reconstruction

Experimental study
Contrast

Contrast to Noise Ratio

- Measured from numerical simulations
  - 2 x 2 cm phantom with high density of scatterers
  - 8mm-diameter anechoic lesion centered inside the phantom

Reconstruction results

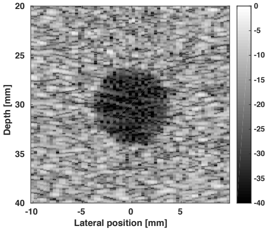

(a) Classic reconstruction

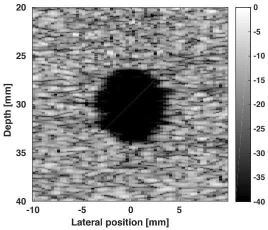

(b) Sparse reconstruction

Contrast to Noise Ratio

- Measured from numerical simulations
  - 2 x 2 cm phantom with high density of scatterers
  - 8mm-diameter anechoic lesion centered inside the phantom

Reconstruction results

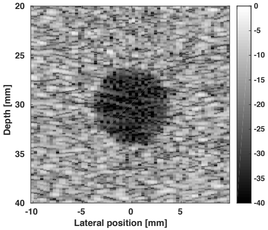

(a) Classic reconstruction

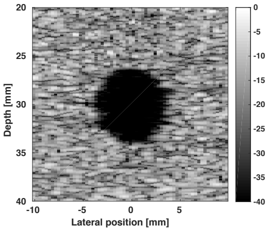

(b) Sparse reconstruction

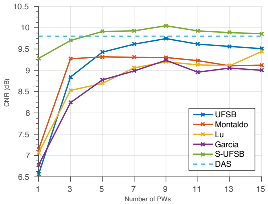

(c) CNR comparison with compounding

ÉCOLE POLYTECHNIQUE FÉDÉRALE DE LAUSANNE

Experimental data

- Using the UlaOp system with a linear probe (64 elements, 5MHz center frequency, 50MHz sampling frequency)
- Measured at different depths

Experimental study
Spatial Resolution

Experimental data

- Using the UlaOp system with a linear probe (64 elements, 5MHz center frequency, 50MHz sampling frequency)
- Measured at different depths

Reconstruction results

Experimental data

- Using the UlaOp system with a linear probe (64 elements, 5MHz center frequency, 50MHz sampling frequency)
- Measured at different depths

Reconstruction results

Experimental study
Spatial Resolution

Experimental data

- Using the UlaOp system with a linear probe (64 elements, 5MHz center frequency, 50MHz sampling frequency)
- Measured at different depths

Reconstruction results

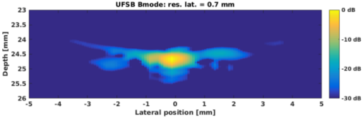

(a) Classic reconstruction

Experimental study
Spatial Resolution

Experimental data

- Using the UlaOp system with a linear probe (64 elements, 5MHz center frequency, 50MHz sampling frequency)
- Measured at different depths

Reconstruction results

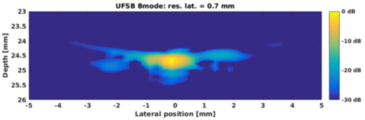

(a) Classic reconstruction

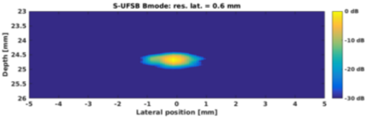

(b) Sparse reconstruction

Experimental data

- Using the UlaOp system with a linear probe (64 elements, 5MHz center frequency, 50MHz sampling frequency)
- Measured at different depths

Reconstruction results

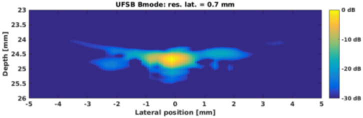

(a) Classic reconstruction

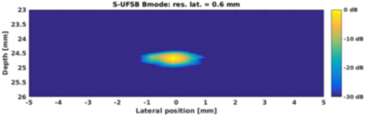

(b) Sparse reconstruction

Depth	Lu		Garcia		UFSB		Montaldo		S-UFSB	
	Axial	Lateral	Axial	Lateral	Axial	Lateral	Axial	Lateral	Axial	Lateral
25 mm	0.4 mm	0.7 mm	0.4 mm	0.6 mm	0.4 mm	0.7 mm	0.4 mm	0.6 mm	0.3 mm	0.6 mm
35 mm	0.7 mm	0.7 mm	0.7 mm	0.7 mm	0.7 mm	0.7 mm	0.7 mm	0.7 mm	0.5 mm	0.6 mm
45 mm	0.6 mm	1 mm	0.6 mm	1 mm	0.6 mm	0.9 mm	0.6 mm	1 mm	0.6 mm	1 mm

(c) Spatial resolution from UlaOp scanner

Outline

Conclusions and perspectives

New reconstruction method

Conclusions and perspectives

New reconstruction method

- Exploits sparsity of US images to solve the inverse problem

Conclusions and perspectives

New reconstruction method

- Exploits sparsity of US images to solve the inverse problem
- Yields better image quality

Conclusions and perspectives

New reconstruction method

- Exploits sparsity of US images to solve the inverse problem
- Yields better image quality
- High computational load at reconstruction

Conclusions and perspectives

New reconstruction method

- Exploits sparsity of US images to solve the inverse problem
- Yields better image quality
- High computational load at reconstruction

Perspectives

Conclusions and perspectives

New reconstruction method

- Exploits sparsity of US images to solve the inverse problem
- Yields better image quality
- High computational load at reconstruction

Perspectives

- Extension to all the Fourier methods (Garcia and Lu)

Conclusions and perspectives

New reconstruction method

- Exploits sparsity of US images to solve the inverse problem
- Yields better image quality
- High computational load at reconstruction

Perspectives

- Extension to all the Fourier methods (Garcia and Lu)
- Acceleration and optimization of the current algorithms (GPU implementation)

Conclusions and perspectives

New reconstruction method

- Exploits sparsity of US images to solve the inverse problem
- Yields better image quality
- High computational load at reconstruction

Perspectives

- Extension to all the Fourier methods (Garcia and Lu)
- Acceleration and optimization of the current algorithms (GPU implementation)
- Extension of the framework to diverging waves

Conclusions and perspectives

New reconstruction method

- Exploits sparsity of US images to solve the inverse problem
- Yields better image quality
- High computational load at reconstruction

Perspectives

- Extension to all the Fourier methods (Garcia and Lu)
- Acceleration and optimization of the current algorithms (GPU implementation)
- Extension of the framework to diverging waves

THANK YOU FOR YOUR ATTENTION!

ADMM algorithm

- The general problem we solve is the following one:

$$\min_{\bar{\boldsymbol{x}} \in \mathbb{C}^N} f\left(\bar{\boldsymbol{x}}\right) \text{ subject to } h\left(\boldsymbol{y} - \Phi \bar{\boldsymbol{x}}\right) = 0, \tag{1}$$

- The ADMM algorithm is:

Input: k $= 0$, choose $\boldsymbol{x}^{\mathbf{0}}$, $\boldsymbol{z}^{\mathbf{0}}$, $\boldsymbol{\lambda}^{\mathbf{0}}$, $\mu > 0$, $\gamma > 0$

1: **repeat**

2: $\quad \boldsymbol{z}^{(t+1)} = \mathrm{prox}_{\gamma h}(\boldsymbol{y} - \Phi \boldsymbol{x}^{(t)} - \boldsymbol{\lambda}^{(t)})$

3: $\quad \boldsymbol{x}^{(t+1)} = \mathrm{prox}_{\mu\gamma f}\left(\boldsymbol{x}^{(t)} - \mu \Phi^H \left(\boldsymbol{\lambda}^{(t)} + \Phi \boldsymbol{x}^{(t)} - \boldsymbol{y} + \boldsymbol{z}^{(t+1)}\right)\right)$

4: $\quad \boldsymbol{\lambda}^{(t+1)} = \boldsymbol{\lambda}^{(t)} + \beta \left(\Phi \boldsymbol{x}^{(t+1)} - \boldsymbol{y} + \boldsymbol{z}^{(t+1)}\right)$

5: **until** A stopping criterion is met